Surface Science 77 (1978) 283–300

DIFFUSE LEED INTENSITIES OF DISORDERED CRYSTAL SURFACES

IV. Application of the disorder theory

D. WOLF, H. JAGODZINSKI and W. MORITZ
Institut für Kristallographie und Mineralogie der Universität München, Theresienstrasse 41, D-8000 München 2, Germany

Received 5 August 1977; manuscript received in final form 3 April 1978

The principles of the statistical disorder theory are discussed briefly. The theory is applied to a model of the disordered (101)Au surface with the characteristic (1 × 2) superstructure. A fit procedure is described, by which the experimental angular intensity profiles are used directly to determine the disorder parameters and the interaction energies between the chains of surface atoms.

1. Introduction

The results of diffraction experiments with low energy electrons on (101)Au surfaces have been described in part III of this series of papers [1]. The observed (1 × 2) superstructure patterns and the distinct broadening of the reflexes in [010] direction can be explained only by assuming irregularities of the surface periodicity. This example of a one-dimensionally disordered surface structure is well suited for an application of the theoretical results developed in parts I and II [2,3]. The principles of this theory will be repeated here only very briefly.

Using a pseudokinematic approximation the disorder parameters can be determined directly by an analysis of the angular beam profiles. Some approximate assumptions have to be made in order to reduce numerical calculations. The most effective reduction is the limitation of the area of multiple scattering (AMS) and of the area of thermodynamical interactions (ATI). Only nearest neighbors are included in this analysis and it has been checked by model calculations with the multiple scattering theory [4] that this approximation is sufficient. It has been pointed out in part I that the inclusion of a larger AMS does not involve any difficulty. Consequenctly, the data analysis outlined below remains to be valid as long as the ATI is not increased.

The (1 × 2) superstructure of the Au(110) surface is most probably caused by a rearrangement of the gold atoms in the uppermost layer. No impurities could be detected by Auger electron spectroscopy measurements. Several models can be

offered to explain the (1 X 2) superstructure. Some of them, which assume a flat surface i.e. a shifting of adjacent chains parallel to the surface, can be excluded by arguing that at constant temperature a variation of the half-widths of the diffuse beams with varying energy and angle of incidence of the primary beam is observed in the experiment. It may be shown that such a variation of the half-widths indicates a roughened or stepped surface, that means, equivalent structural elements with the same effective scattering amplitude occur in different heights normal to the surface; this is valid even in the case of a complete multiple scattering calculation.

Here we choose the most simple model where rows of atoms parallel to the $[10\bar{1}]$ direction are missing or added. It can be understood as a first stage of facetting to (111) faces. Of course, with the aid of the method applied here, no direct structure determination is correlated. It is only the sequence of structural elements that is determined uniquely. Obviously these parameters are consistent with several possible structure models fulfilling the conditions mentioned above.

2. Review of the main principles

A detailed description of the disorder theory is given in part I and II of this report. All necessary assumptions have been discussed, especially for the application in LEED. Therefore, the general principles of this theory will only be outlined here.

For a one-dimensionally disordered lattice the equation for the diffracted intensity is given by:

$$I(\boldsymbol{k}, \boldsymbol{k}') = R \sum_{j}^{-(N_2-1),(N_2-1)} (N_2 - |j|)\, \langle FF_j^*(\boldsymbol{k}, \boldsymbol{k}') \rangle \exp(-ijA_2) \sum_{g_x} \delta(K_x' - K_x - g_x)\,,$$

$$A_2 = (\boldsymbol{k}' - \boldsymbol{k}) \cdot \boldsymbol{b} \hat{=} 2\pi K\,. \qquad (1)$$

The vectors $\boldsymbol{a}$ and $\boldsymbol{b}$ of the surface unit cell are in the directions x and y, the direction z is normal to the surface; y is chosen to be the direction of the one-dimensional disorder, the defects in the x-direction are neglected, i.e., the undisturbed lattice periodicity in this direction causes sharp reflexes.

The significance of the diverse factors is explained in part I and II. The determination of the unknown average $\langle FF_j^* \rangle$ is the central problem in the analysis of disordered structures.

The calculation of $\langle FF_j^* \rangle$ for a hypothetical structure model is possible in principle for X-rays as well as low energy electrons; however, in the case of LEED, the multiple scattering processes have to be considered.

The calculation of the angular profiles of LEED reflexes is practicable only if statistical parameters are determined experimentally; a trial and error determination of the mean value $\langle FF_j^* \rangle$ needs too much computation effort because of the compli-

cated calculation of exact atomic scattering factors F_ν and the multiple scattering of slow electrons.

The disorder theory applied here to LEED results contains a procedure for the experimental determination of the statistical parameters by intensity measurements. It may be shown that this approach is valid as long as a linear expansion of the averaged structure factor $\langle F,F_j^*(\boldsymbol{k},\boldsymbol{k}')\rangle$ at the position of the maximum of the beam profile is a good approximation to its dependence on the scattering angle. This assumption is valid approximately in a certain range of the intensity curve I versus the scattering angle θ.

For the calculation of the average $\langle FF_j^*\rangle$ at first the probabilities $p_{mn}(1)$ for the succession of chains with the generalized structure amplitude $F(\boldsymbol{k},\boldsymbol{k}')$ are defined. The $F(k,k')$ contain the sum over layers:

$$F_m(\boldsymbol{k},\boldsymbol{k}') = \sum_\nu f_{\nu,m}(\boldsymbol{k},\boldsymbol{k}') \exp[\mathrm{i}(\boldsymbol{k}-\boldsymbol{k}')\cdot\mathbf{d}_\nu] \,.$$

The average we are looking for may be expressed in the following form:

$$\langle F,F_j^*(\boldsymbol{k},\boldsymbol{k}')\rangle = \sum_m \sum_n p_m p_{mn}(j)\, F_m F_n^*(\boldsymbol{k},\boldsymbol{k}') \,, \tag{2}$$

with the parameters: p_m = probability to find a chain with the generalized structure amplitude F_m, and $p_m p_{mn}(j)$ = probability to find a pair of chains with structure amplitudes F_m and F_n at the distance $j\,\boldsymbol{b}$, where $\boldsymbol{b}$ is the lattice spacing in the direction of disorder for which the general relations derived in part I are valid.

The probabilities $p_{mn}(j)$ are related to the sequence of chains and depend on the number of different configurations, that is, how many different F_m are used in the data analysis. On the other hand, the sequence of chains is a function of the interaction energies and the temperature. To avoid confusion with employed probabilities p_{mn} introduced above, we shall call this set of probabilities, which is determined by thermodynamical quantities, α_m. The probabilities α_m describe the state of order of the surface. Of course, a simple relation exists between the p_{mn} and α_m.

The probabilities $p_{mn}(j)$ can either be calculated according to the method of the difference equation, i.e., by determining a recursive formula for the $p_{mn}(1)$, or according to the matrix method, i.e., by the formation of a matrix from the sequence probability [5,6]. The two methods lead to the inhomogeneous equation of the degree r:

$$p_m p_{mn}(j) = \sum_r C_{mn}^{(r)} \lambda_r^j \,, \tag{3}$$

in which λ_r are the eigenvalues of the matrix $p(1)$. The constants $C_{mn}^{(r)}$ are given in a complicated manner by products of the p_{mn} and λ_r divided by products of the differences of $\lambda_\nu - \lambda_r$. Consequently, the constants may have the value 0/0. These cases need a detailed investigation of the range of diffraction angles and electron energies concerned. The reconsideration yields a solution of the problem in any

case. The degree r of the inhomogeneous equation depends on the parameters p_{mn} as well as on the area of direct thermodynamical interaction of the different chains in the structure model. Solving the homogeneous equation

$$|P(1) - \lambda E| = 0 ,$$

the eigenvalues λ_1 to λ_N are determined.

Hence follows the general solution for the average $\langle FF_j^* \rangle$:

$$\langle FF_j^*(k, k') \rangle = \sum_r K_r(k, k') \lambda_r^j , \quad \lambda_r = |\lambda_r| \exp(i\phi_r) = \rho_r \exp(i\phi_r) ,$$

$$K_r(k, k') = \sum_{m,n} C_{mn}^{(r)} F_m F_n^*(k, k') = B_r(k, k') + iD_r(k, k') . \tag{4}$$

The final formula for the intensity backscattered from a one-dimensionally disordered surface lattice is obtained inserting (4) into (1)

$$I(k, k') = R \left[\sum_r^{1,N} \left(B_r \frac{1 - |\lambda_r|^2}{1 - 2|\lambda_r| \cos(A_2 + \phi_r) + |\lambda_r|^2} \right.\right.$$

$$\left.\left. - 2D_r \frac{|\lambda_r| \sin(A_2 + \phi_r)}{1 - 2|\lambda_r| \cos(A_2 + \phi_r) + |\lambda_r|^2} \right) \right] \delta(K_x - K_x' + g_x) . \tag{5}$$

If one eigenvalue is $|\lambda| = \pm 1$ at the position of maximum, the corresponding term of the sum represents a sharp spot according to the two-dimensional lattice factor of the undisturbed lattice; the first term in the sum of (5) represents a symmetric part of the profile of the diffuse interferences; the second one describes an asymmetric contribution. At the transition into the undisturbed or strictly ordered atomic arrangement, all non-vanishing eigenvalues λ_r will become 1, and the equation changes to the well known expression for the diffracted intensity backscattered from ideal crystals

$$I_R = I_0 |G|^2 |F|^2 ,$$

with the usual lattice factor G and the generalized structure amplitude F.

Therefore, the intensity distribution of the beam profiles of disordered surfaces depends on the following disorder parameters:

(a) The functions B and D, containing the generalized structure amplitude F of the scattering complexes, have an essential influence upon the intensity distribution. As far as X-ray diffraction is concerned, the disorder problem is generally solved with the aid of the F data available, i.e., theoretical curves can be compared with experimental measurements. In the pseudokinematic analysis of LEED data the parameters B and D are approximated as described below, over the angular range of the beam profile. The eigenvalues λ_r are derived from the full width at half maximum and the parameters B and D are determined by fitting the experimental beam profile.

(b) The eigenvalues λ_r are connected with the sequence probabilities α_m, which

determine the width of the intensity profiles. The relation,

$$\alpha = \exp(-\Delta V/kT)/2\cosh(\Delta V/kT)\,,$$

describes the probabilities α_m with the difference of the interaction energies V of the scattering complexes; consequently, a direct relation between interaction energies and profile width exists [2].

(c) Each beam corresponds to an eigenvalue λ_r;

$$A_2 + \phi_r = (k' - k)\cdot b + \phi_r = 2\pi k + \phi_r\,,$$

ϕ_r determines the positions of the diffuse beams in relation to the integer order beams; k is the usual Miller index in the b^* direction of the reciprocal lattice. In the case of half-order reflections, $\phi_r = \pi$, and λ_r is negative.

These principles of the disorder theory – which had originally been developed for the analysis for the diffuse X-ray diffraction patterns – are extensively described in the corresponding special literature [5,6], and with modifications for LEED in Parts I and II.

3. Model of a roughened (101) surface

LEED observations of the (101)Au surface show a (1 X 2) superstructure with diffuse reflexes. Since no surface contamination by impurity atoms could be detected with the aid of Auger electron spectroscopy, the following surface model can be suggested.

The (101) surfaces of the face-centered cubic gold consist of rows of atoms parallel to the $[10\bar{1}]$ direction, fig. 1a.

By addition or removal of single chains the surface will be roughened, fig. 1b. As a consequence of this roughening process the rows of atoms may occur in different heights. The (1 X 2) superstructure is caused by periodic gaps in the arrangement of chains. Chains of impurity atoms filling the gaps with a corresponding scattering factor cannot be excluded, but will not be taken into consideration at the moment.

Along the close-packed $[10\bar{1}]$ direction the rows are almost perfectly ordered. The lattice constant is doubled in the [010] direction by removing every second chain, however, no strict periodicity is realised because of statistical faults in the sequence of rows.

Assuming only nearest neighbor interactions and, that the area of multiple scattering is restricted to the same range, the disorder problem can be formulated as follows:

The statistics of the surface model contain four different types of chains, which may occur in different heights above or below the average level of the surface. The type of the chain is determined by its surroundings. The probability that one chain with the scattering factor F_1 is followed by another one with F_2 is given by $p_{12}(1) = \alpha_1$; then $p_{13}(1) = 1 - \alpha_1$ is the probability for a succession F_1F_3. All

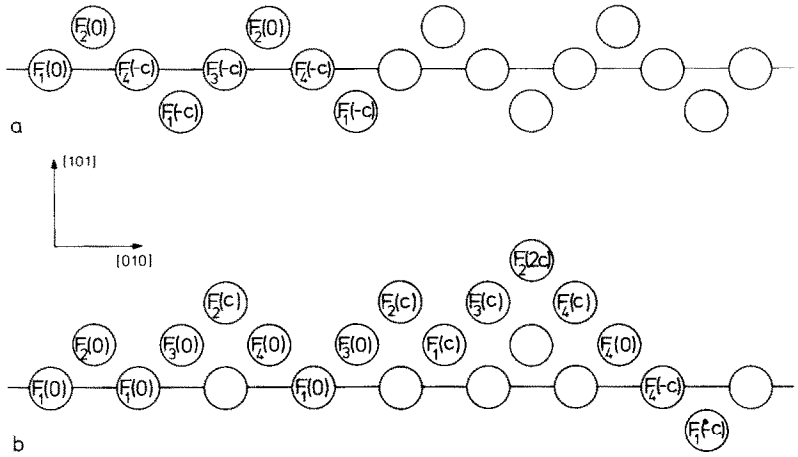

Fig. 1. (0*kl*) cross section of the (101)Au surface: (a) ordered structure; (b) roughened surface.

further α_m, which are necessary for the calculation of the beam profile, are defined analogically. In addition to the partial waves, a phase factor

$$[\exp(\mathrm{i}\varphi) = \exp[\mathrm{i}(k_\perp - k'_\perp)\, c]$$

must be added to such chains which are shifted against the normal positions on the zero line level; c is the distance between the layers which is postulated to be constant. It is practical to include the phase factor $e^{i\varphi}$ in the matrix of probabilities, that means, the matrix $p(1)$ becomes complex.

The dependence of interaction energies V_{ik} and the probabilities are given by:

$$\alpha_1 = \exp(-\Delta V_1)/2\cosh \Delta V_1 \quad \alpha_2 = \exp(-\Delta V_3)/2\cosh \Delta V_3\,, \tag{7}$$

with

$$\Delta V_1 = (V_{13} - V_{12})/2kT\,, \quad \Delta V_3 = (V_{33} - V_{32})/2kT.$$

A simplified solution of the problem can be obtained, if the interaction energies are considered to be symmetrical, fig. 1b:

$$V_{12} = V_{21}\,, \quad V_{13} = V_{24}\,, \quad V_{32} = V_{41}\,, \quad V_{33} = V_{44}\,.$$

These symmetry relations are not valid if the surface is contaminated by foreign atoms with different sticking coeffients for the various types of chains, i.e. an atom is adsorbed more probably on a chain F_1 than on F_2 or F_3.

The phase factors of the probabilities α_m are changed if the statistical order of succession is inverted.

Therefore, two different schemes for the sequence probabilities α_m can be defined:

(a) for the positive direction:

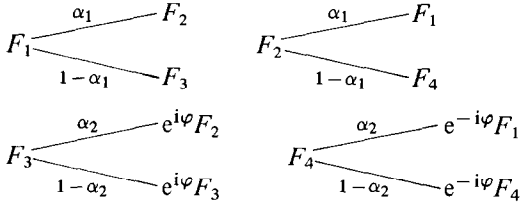

(b)

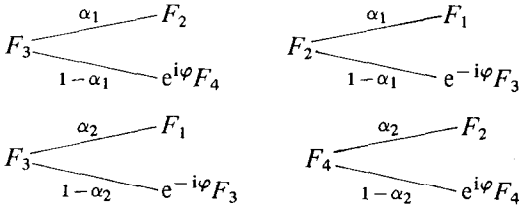

Of course both schemes result in the same equation for the eigenvalues:

$$\begin{vmatrix} -\lambda & \alpha_1 & 1-\alpha_1 & 0 \\ \alpha_1 & -\lambda & 0 & 1-\alpha_1 \\ 0 & e^{i\varphi}\alpha_2 & -\lambda + (1-\alpha_2)\, e^{i\varphi} & 0 \\ e^{-i\varphi}\alpha_2 & 0 & 0 & -\lambda + (1-\alpha_2)\, e^{-i\varphi} \end{vmatrix} = 0 . \tag{8}$$

The solution of this determinant leads to the equation:

$$\lambda^4 - 2(1-\alpha_2)\cos\varphi\,\lambda^3 - [\alpha_1^2 - (1-\alpha_2)^2]\,\lambda^2 + 2\alpha_1(\alpha_1 - \alpha_2)\cos\varphi\,\lambda - (\alpha_2 - \alpha_1)^2 = 0 . \tag{9}$$

The eigenvalues λ_r as a function of the probabilities α_1 and α_2 have been calculated solving eq. (9) numerically. Comparison with the observed eigenvalues $|\lambda_{r\,\mathrm{obs}}|$ determines the experimental values α_1 and α_2. $|\lambda_{r\,\mathrm{obs}}|$ were obtained fitting the theoretical beam profiles to the experimental ones.

Four different types of order may be defined by variation of α_1 and α_2:

(1) $\alpha_1 \to 0, \alpha_2 \to 1$:

a periodic structure $F_1F_3F_2F_4\overline{F_1F_2F_3F_4}$ ... is approached;

(2) $\alpha_1 \to 1, \alpha_2 \to 1$:

a periodic structure $F_1F_2\overline{F_1F_2}$ ... is realized, which corresponds to the normal (1 X 1) structure of the (101) surface;

(3) $\alpha_1 \to 0, \alpha_2 \to 0$:

we have a mixture of periodic sequences $F_3\bar{F}_3$... and $F_4\bar{F}_4$...;
(4) $\alpha_1 \to 1, \alpha_2 \to 0$:
a mixture of 3 periodic structures $F_1F_2\overline{F_1F_2}$ ...., $F_3\overline{F_3}$..., and $F_4\bar{F}_4$ is approached (facets and periodic microfacets).

In intermediate states of disorder a more or less statistical or even random order of chains is realized. Because of the surface equilibrium condition large step heights are excluded. Apparently the probability α_2 must be given by $0.5 < \alpha_2 < 1$, otherwise a completely disordered surface structure or another superstructure with a different lattice constant would be observed, that means, the surface roughening is small and the probabilities for chain sequences F_3–F_3 and F_4–F_4 are low.

4. Analysis of the beam profiles

The eigenvalues λ_r and the sequence probabilities α_m have been determined by analyzing the deconvoluted beam profiles (see part III).

The functions

$$u(\rho) = \frac{1-\rho^2}{1-2\rho\cos(2\pi k+\Phi)+\rho^2}\,,$$
$$v(\rho) = \frac{\rho\sin(2\pi k+\Phi)}{1-2\rho\cos(2\pi k+\Phi)+\rho^2}\,, \tag{12}$$

are used to fit the experimental profiles by variation of ρ.

From eq. (8) we get four eigenvalues $\lambda_r = \rho_r \exp(i\Phi_r)$; two of them are real, the remaining two imaginary. The periodicity in [010]* is doubled, as we took in eq. (5) the distance between the chains as lattice constant.

Therefore the eigenvalues generate for $\Phi = \pi/2, 3\pi/2, \ldots$ the $(0, k/2)$ superstructure beams in the positions $k = 1/2, 3/2, \ldots$. For $\Phi = 0, \pi, 2\pi, \ldots$ the eigenvalues λ become real and describe the $(0, k)$ beams in the positions $k = 0, 1, 2, \ldots$.

The diffuseness of the reflections is a function of the energy and changes from the $(0, k/2)$ superstructure beams to the integer order beams and vice versa, if the energie varies. Here only the measurements at constant energy are evaluated.

First of all, eigenvalues λ_r have been estimated by calculating the values of the function $u(\rho)$ in the range $0.1 \leqslant \rho \leqslant 0.9$ and plotting the curve versus k ($A_2 = 2\pi k$) (fig. 2a). With the full width at half maximum (FWHM) of these curves a calibration curve ρ(FWHM) has been determined (fig. 2b); analogically the calibration curve for the maximum position of the asymmetric function $v(\rho)$ has been ascertained (figs. 2c and 3d).

By comparing the FWHM β of the deconvoluted experimental profile with the ρ(FWHM) curve an approximate λ value may be estimated. Refined eigenvalues $\lambda = \rho\ e^{i\varphi}$ have been determined by fitting the theoretical to the experimental

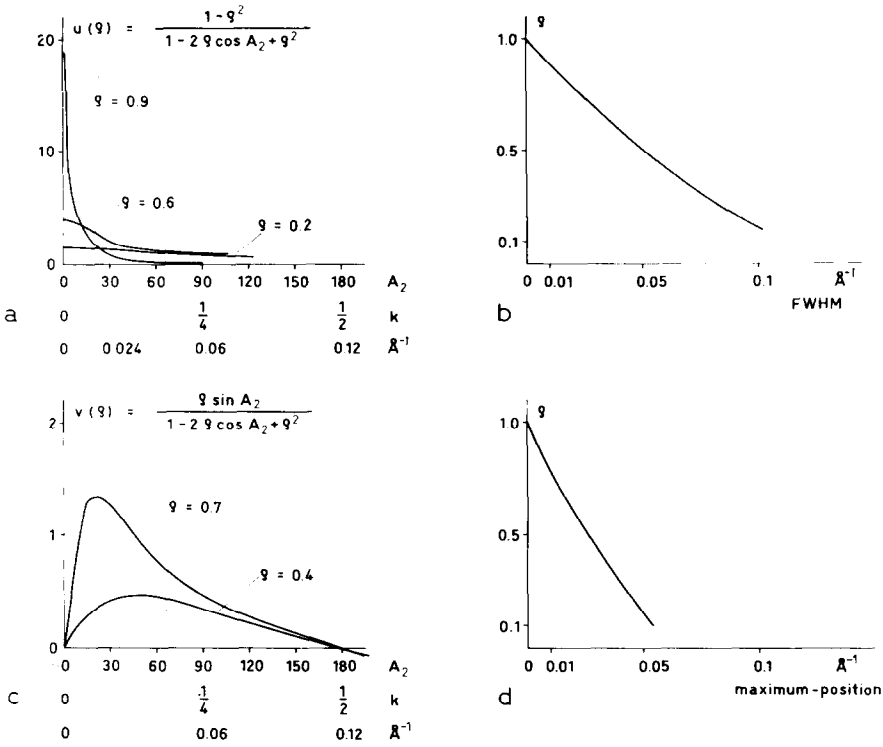

Fig. 2. Calibration curves for ρ and the full width at half maximum of the reflex profiles.

curves. Two examples for crystal temperatures of $T = 25°C$ and $T = 140°C$ are shown in fig. 3.

The maximum of $u(\lambda)$ is calibrated to the maximum of the deconvoluted beam profile; by a similar fit to the experimental curve the asymmetric contribution to the beam has been determined from the function $v(\lambda)$.

In this way eight intensity profiles of the (01) and the $(0\frac{1}{2})$ beams respectively have been evaluated for crystal temperatures within the range of 298 to 858 K. The data for the eigenvalues $|\lambda(T)_{0bs}|$ and the calibration factors B and D are given in table 1. Within the range of crystal temperature $298 < T < 670$ K, the eigenvalues $|\lambda_{obs}|$ correspond to the λ_{cal}; for temperatures $T > 670$ K the $(0\frac{1}{2})$ beam disappears gradually and the validity of the surface model becomes doubtful. This point is carefully discussed in the next section.

The factor $\cos\varphi$ in eq. (9) is determined by $\varphi = (k_\perp - k'_\perp)c$.

The phase factor φ is a critical variable for the beam profile which broadens or sharpens as a function of energy, what may well be observed in the LEED pattern. The inner potential and the upmost layer distance as well change the phase factor φ.

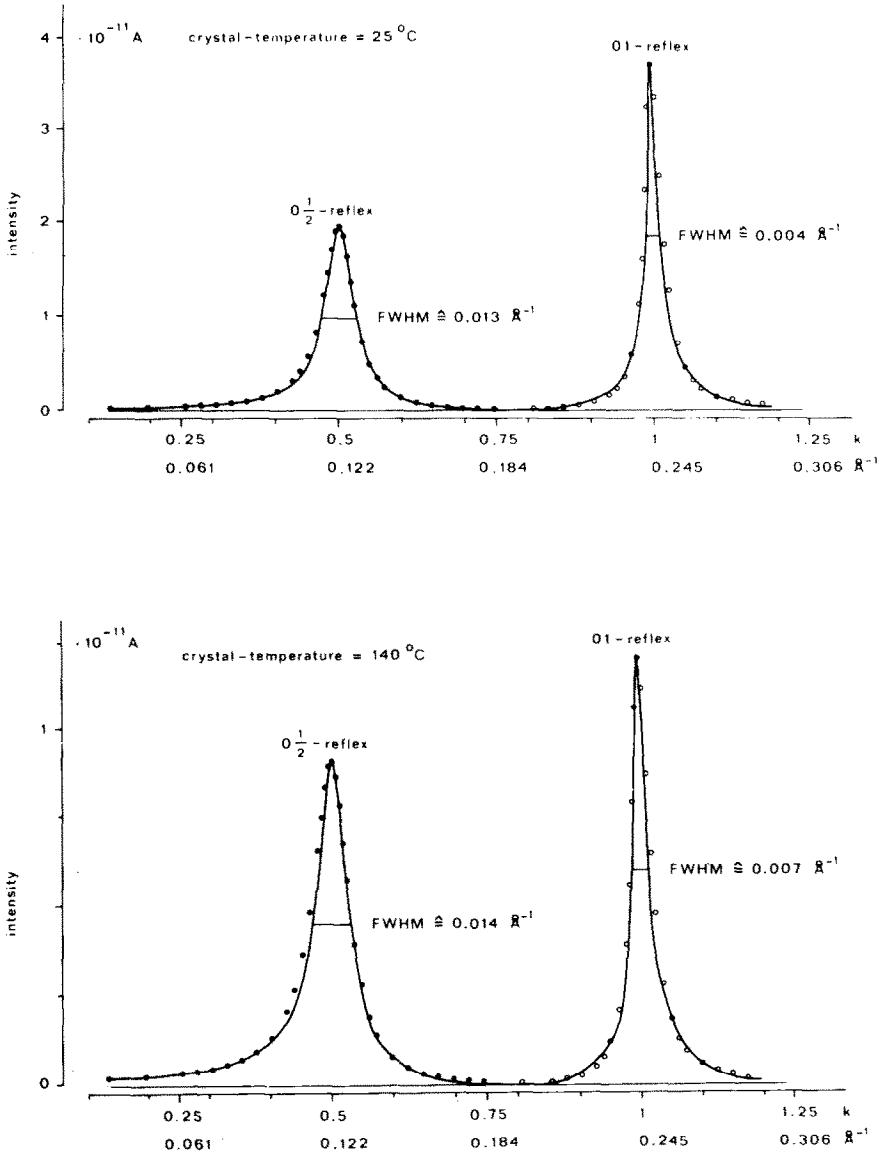

Fig. 3. Comparison of two deconvoluted experimental beam profiles with the fitted curves. Crystal temperatures 25 and 140°C.

Assuming an inner potential, $V_0 = 5$ eV and the bulk distance $c = 1.44$ Å, the best fit was achieved. It should be noted that no exact determination of the binding distances of the surface atoms has been tried here. This would indeed include the

Table 1

	Temperature		$\lvert\lambda_{obs}\rvert$	B	D	λ_{cal}		$\lvert\lambda_{cal}\rvert$	α_1	α_2
	(°C)	(K)				Re	Im			
O1 reflex	25	298	0.90	9.82	0.8	−0.892	–	0.892	0.226	0.94
	140	413	0.89	3.40	0.5	−0.881	–	0.881	0.268	0.945
	245	518	0.88	2.23	0.4	−0.875	–	0.875	0.296	0.95
	300	573	0.87	1.90	0.2	−0.872	–	0.872	0.306	0.95
	400	673	0.87	1.10	0.2	−0.865	–	0.865	0.34	0.955
	440	713	0.86	0.76	0.1	−0.85	–	0.85	0.45	0.975
	500	773	0.82	0.60	0.08	–	–	–	–	–
	585	858	0.78	0.37	0.06	–	–	–	–	–
O_2^1 reflex	25	298	0.83	9.11	1.0	0.055	−0.835	0.837	0.226	0.94
	140	413	0.80	4.9	0.95	0.07	−0.807	0.810	0.268	0.945
	245	518	0.80	3.81	0.71	0.08	−0.79	0.794	0.296	0.95
	300	573	0.78	3.17	0.65	0.08	−0.78	0.784	0.306	0.95
	400	673	0.74	1.30	0.28	0.09	−0.745	0.750	0.34	0.955
	440	713	0.66	0.90	0.16	0.13	−0.66	0.67	0.45	0.975
	480	753	0.51	0.67	0.12	–	–	–	–	–
	515	788	0.42	0.56	0.11	–	–	–	–	–

exact calculation of multiple scattering amplitudes and the comparison of calculated $I(E)$ curves with measured ones. Here only the statistical parameters are determined.

The calculated values for $\lambda_{r\,\mathrm{theor}}$ and α_1, α_2 are summarized in table 1. The probabilities α_m describe the degree of the surface disorder quantitatively. Therefore the values α_m of the $(0, k)$ and the $(0, k/2)$ beams must agree within the experimental limit of error. Only in this case the two disorder parameters determined separately describe the same order.

5. Conclusions

The dependence of the integrated intensity of the (01/2) reflex as a function of the temperature can be extrapolated to an approximate critical temperature $T_c \approx$ 420°C (713 K) (fig. 4).

The exponential relation (6), modified here by substituting ΔV:

$$\alpha(T) = \frac{\exp[-L(T)\,\Delta F/2kT]}{2\cosh L(T)\,\Delta F/2kT}, \tag{13}$$

where $\Delta F = \Delta U - T\Delta S$, F = free energy, U = potential energy, and S = entropy, is confirmed by the probability α_1; $L(T)$ is a factor, which corresponds to the averaged chain length, which has to be introduced on account of the simplified one-dimensional model. The entropy S may represent some disorder on internal heat. In a strict sense U and S are temperature dependent. A logarithmic plot of $\alpha_1(T)$ versus T shows a straight line with a changed slope at $T > T_{\mathrm{crit}}$. For temperatures above 740 K the surface state changes drastically and other interaction energies result. The ordinate value of the straight line fig. 5 can be explained only by introducing the free energy F, if U is considered to be independent of T in a first approximation; consequently the entropy term plays an important role and cannot be neglected as originally assumed. From the slope and the ordinate intersection of

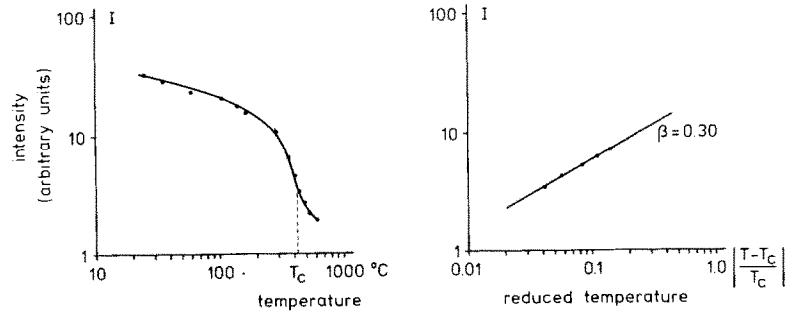

Fig. 4. Integral intensity of the $0\frac{1}{2}$ beam as a function of temperature and reduced temperature.

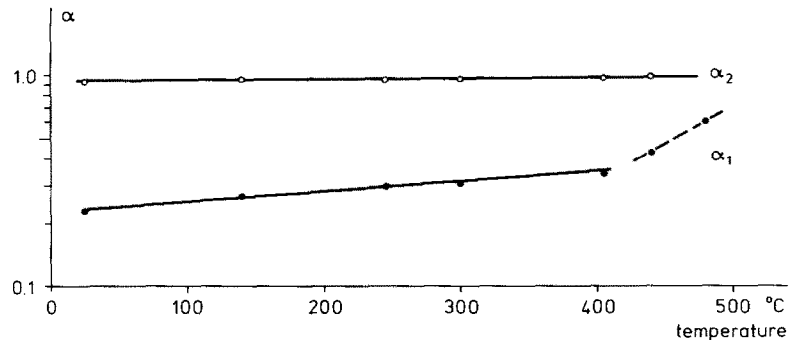

Fig. 5. Sequence probabilities α_1 and α_2 as a function of temperature.

the straight line the energy values summarized in table 2 have been determined.

The difference of free energies ΔF as a function of temperature is shown in fig. 6. We notice that the model of the roughened (101) gold surface is valid unrestrictedly for temperatures below T_{crit} or $L(T) = \text{constant}$; energy values determined above this temperature are not relevant to the model, i.e., because of the dissociation of the chains, that means a decrease of the average chain length. This is in agreement with the diffraction pattern, which shows a sudden increase of the line width of the diffuse streaks, what has to be interpreted in terms of a corresponding decrease of the chain length $L(T)$.

The energy values ΔF, as determined from the beam profiles, confirm the model:

As mentioned above, the probabilities α_1, α_2 are functions of the differences in free energy ΔF_i of the complexes; the slope and ordinate value of the straight line $\alpha(F)$ plotted logarithmically are proportional to the interaction energy ΔU and the entropy ΔS respectively. According to eq. (13), ΔU and ΔS should be proportional

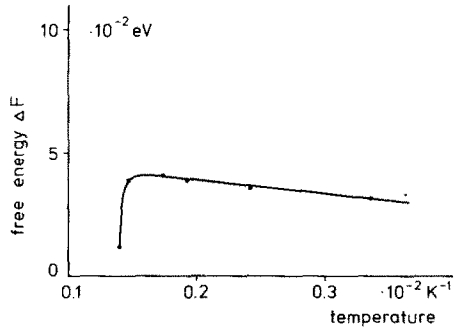

Fig. 6. Free energy ΔF of the chains as a function of temperature.

Table 2

Temperature		U	S	TS	$\log \frac{\alpha_1}{1-\alpha_1}$	U	F
(K)	(10^{-2} K^{-1})	(10^{-2} eV)	(10^{-5} eV deg^{-1})	(10^{-2} eV)		(10^{-2} eV)	(10^{-2} eV)
298	0.336	2.18	−3.07	0.91	−0.535	2.25	3.16
413	0.242			1.27	−0.436	2.3	3.57
518	0.193			1.59	−0.376	2.27	3.86
573	0.174			1.76	−0.356	2.29	4.05
673	0.147			2.08	−0.288	1.79	3.87
713	0.140			2.19	−0.087	−0.95	1.24

to the average length $L(T)$ of the chains parallel [101], which is temperature dependent. Now we discuss the meaning of the average chain length in our disordered model structure.

As shown in fig. 7, the ordered superstructure may be realized in two ways differing by a translation of the unit length in [010] of the surface lattice. In terms of the description for three-dimensional crystals these domains are antiphase domains with a translation vector [010] of the supercell. Below the critical temperature T_c, the length of these chains should therefore be infinite (no antiphase domains). Therefore, we should have $\alpha_1 \to 0$ below the critical temperature. As α_1 is approximately 0.2 at room temperature, there is a considerable number of defects even at temperatures appreciably lower than T_c. This can only be explained by assuming antiphase domains or other types of defects destroying the long-range order of chains. The application of a one-dimensional Ising model can only be justified with this assumption. In this particular case, $L(T)$ may be considered to be temperature-independent up to a temperature of T_L below T_c. Assuming that this condition is valid, we can form

$$\frac{\alpha_1}{1-\alpha_1} = \exp\left[-\frac{\Delta F\, L(T_L)}{kT}\right] \quad \text{or} \quad \log\frac{\alpha_1}{1-\alpha_1} = -C\, L(T_L)\,[T^{-1}\Delta U - \Delta S]\,.$$

The assumption seems to be justified as long as the plot $\log[(1-\alpha_1)/\alpha_1]$ versus T

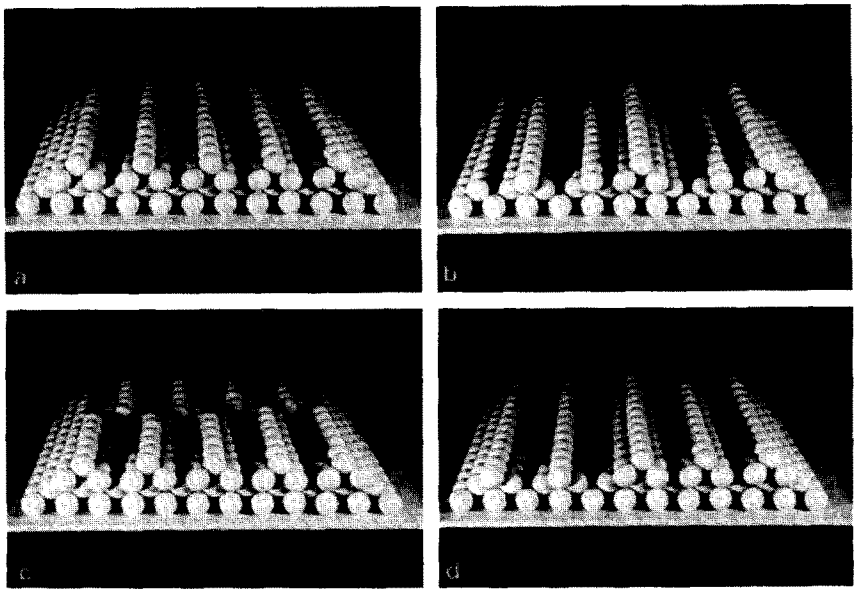

Fig. 7. Model of (110)Au surface: (a) ordered structure; (b) roughened surface; (c), (d) two types of antiphase domains.

yields a straight line, fig. 8. The first significant deviation from a straight line occurs at $T \approx 600$ K.

If this deviation is caused by a decrease of $L(T)$, should be decided by a measurement of the broadness of diffuse lines in the LEED pattern. Unfortunately, the diffuse intensity profiles could only be measured quantitatively parallel to $[010]^*$ for technical reasons. Therefore, the observable change of the diffuseness into $[10\bar{1}]^*$ can be given qualititatively only. Above $T = 670$ K the broadening effect, according to eq. (26) in part I ($L(T) = N_2$), has been observed experimentally by film methods. On the other hand it is possible to extend the plot $\log[(1-\alpha_1)/\alpha_1]$ versus T above the critical temperature. As shown in fig. 8, a straight line with another slope can be detected in this way; the intersection of both lines indicates either a change in the chain length or in the differences of the energies ΔU or the entropies ΔS. This intersection takes place at about $T \approx 680$ K, at a temperature appreciably below T_c, indicating a change of ΔU and ΔS. According to present order–disorder theories the temperature dependence of the integrated intensity of the $(0\frac{1}{2})$ reflex can be used to fix a critical temperature T_c.

From a logarithmic plot of the relation

$$I = C[(T - T_c)/T_c]^{2\beta},$$

the critical temperature T_c and the critical point exponent β can be determined. This plot is shown in fig. 4; it fixes $T_c = 713 \pm 10$ K and $\beta \approx 0.30$. Obviously this plot can only be justified if the critical temperature is known accurately. On the other hand it is well known that the integral intensity may be changed by the temperature factor.

The exact factor cannot be given as long as the theoretical treatment of the scattering problem, including the lattice dynamics at the surface, has not been done successfully.

In a first approximation the integration for reciprocal vectors parallel to the surface should not vary with the temperature; this does not apply to the integrated measurement vertical to the surface.

This is the reason why the usual plot used for X-ray and neutronscattering cannot be applied to LEED patterns unrestrictedly. Therefore, the meaning of β in

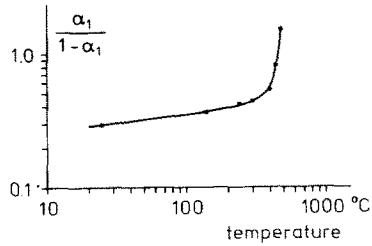

Fig. 8.

comparison ot these measurements must not be overestimated.

Another argument against this plot is the fact already discussed above, that the one-dimensional model may be applied to this transformation, although this model has its critical temperature at $T_c = 0$ K. On the other hand, the critical behaviour of the integral reflex intensity can easily be seen on the diffraction pattern. For this reason it seems to be justified to assume that this critical behaviour is not too much different from the ideal infinite surface. Taking into account all these restrictions one can use the extrapolated curve of $\log[\alpha_1/(1-\alpha_1)]$ versus T for setting the critical temperature T_c. Within the limit of experimental error we get for the critical point exponent

$$0.23 < \beta < 0.37 ,$$

a range which is clearly above the value $\beta = 0.125$ typical for a two-dimensional model.

Buth there is another reason to doubt that the two-dimensional Ising model of disorder is suited to describe disorder phenomena at the surface quantitatively.

As will be shown later, the disorder problem described in this paper may be reduced to the two-dimensional Ising model (rhombic, square lattice) with different, very anisotropic interaction energies ΔU and $\Delta U'$. The critical temperature of this model is given by [7]:

$$\sinh(\Delta U'/kT)\sinh(\Delta U/kT) = 1 . \tag{14}$$

Now we can estimate the average chain length $L(T)$ in the following way: $L(T)$ must be larger than 30 unit cells (no observable line broadening in [010] *) because of the resolution power of the LEED apparatus; the upper limit is unimportant for this discussion.

The maximum energy per unit cell is therefore

$$U' = 2.18 \times 10^{-2} \text{ eV}/30 \approx 7 \times 10^{-4} \text{ eV} ;$$

with

$$kT_c \approx 5 \times 10^{-2} \text{ eV} , \quad \text{we get } U/kT_c < 1.3 \times 10^{-2} .$$

In order to fullfill eq. (14), $\sinh(\Delta U'/\mathrm{kT_c})$ must be larger than 10^2. This again gives a probability of a fault within the approximately ordered chain at T_c of 10^{-4}, which should not change appreciably above T_c. (The short-range order parameter correlated with α_1 is continuous even at T_c.) Buth this small probability is in contradiction – at least by three orders of magnitude – to the diffuseness of reflections observed in [010]* above T_c, which yields a probability larger than 0.1. A more detailed explanation of this argument will be given in a later paper.

This discussion shows that the entropy term introduced in the one-dimensional model structure cannot be assigned to the configurational entropy, caused by the disorder within the chains. Therefore, the only conclusion left is, that the vibra-

tional part of the energy (vibrational entropy) plays an important role in the transformation.

According to table 2 the contribution $-T\Delta S$ to the free energy ΔF of the chains reaches at T_c the same order of magnitude as the contribution of ΔU to ΔF. This means, that at transformation $\Delta F \approx 0$; this again is in agreement with the argument that the surface energies between the two ordered surface states should be equal. This is a classical description of a phase-transformation and means that the free energies assigned to the important configurations are typical for the two structures under discussion. It is also shown experimentally that the surface of a crystal may be regarded as separable thermodynamical phase.

6. Summary

Diffuse LEED intensity profiles of the disordered (1 X 2) superstructure of the (101)Au surfaces are interpreted in terms of a roughened surface. By means of an extended one-dimensional Ising model the intensity profiles of reflections have been calculated and compared with experimental ones. The underlying order–disorder parameters and interaction energies between the chain complexes have been determined as a function of the surface temperature. Below a critical temperature T_c the superstructure is found to be stable; above T_c the chains dissociate and the chain atoms are statistically disordered on a bulk structure substrate.

This method may be generalized for any disorder problem on the surface if the number of scattering complexes involved does not become too large.

Acknowledgement

The authors wish to express their appreciation to the Deutsche Forschungsgemeinschaft for financial support under Sonderforschungsbereich 128.

References

[1] D. Wolf, H. Jagodzinski and W. Moritz, Surface Sci. 77 (1978) ... .
[2] H. Jagodzinski, W. Moritz and D. Wolf, Surface Sci. 77 (1978) ... .
[3] W. Moritz, H. Jagodzinski and D. Wolf, Surface Sci 77 (1978) ... .
[4] W. Moritz, Inst. Phys. Conf. Ser. 41 (1978) 261.
[5] H. Jagodzinski, Acta Cryst. 2 (1949) 201,
[6] H. Jagodzinski, Acta Cryst. 7 (1954) 17.
[7] A.H. Kramers and G.H. Wannier, Phys. Rev. 60 (1941) 252, 263.